π-Electronic Soft Materials Based on Graphitic Nanostructures

T. FUKUSHIMA

[Award Account: SPSJ Wiley Award (2005)]
Vol. 38, No. 8, pp 743–756 (2006)

This paper reviews our recent studies on π-electronic soft materials consisting of graphitic nanostructures. We disclosed novel composite materials consisting of carbon nanotubes and ionic liquids. By programmed self-assembly of graphene-like molecules, we developed non-covalent graphitic nanotubes with tailored electronic functions. One-dimensional columnar assemblies formed from such molecular graphenes can be constructed in the channels of mesoporous silicates. Herein, details of the design, properties, and scope of our materials are described.

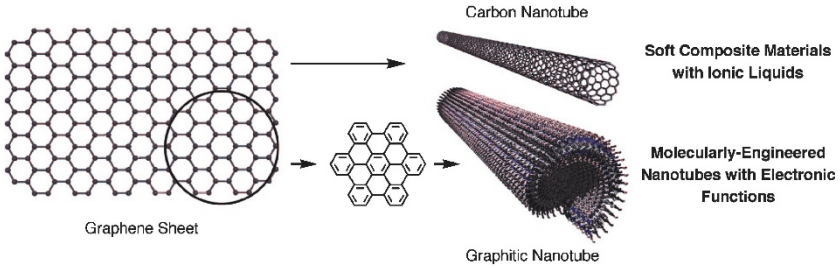

Application of Catastrophe Theory to the Neck-initiation of Semicrystalline Polymers Induced by the Intercluster Links

K. NITTA and M. TAKAYANAGI

[Regular Article]
Vol. 38, No. 8, pp 757–766 (2006)

The necking initiation in semi-crystalline polymers composed of lamellar clusters can be explained by catastrophic phase-transition in the same manner of a first order phase transition of van der Waals gas. Catastrophic arrangement of the intercrystalline links results in sudden emergence of the locally oriented region, leading to the neck formation.

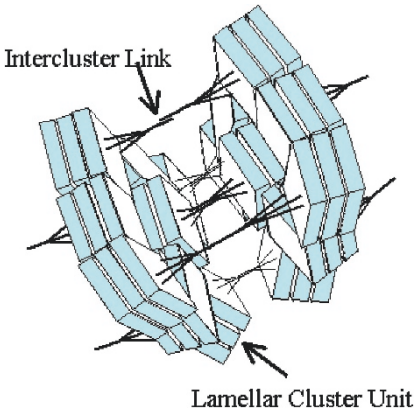

The Effect of Rubber Type and Rubber Functionality on the Morphological and Mechanical Properties of Rubber-toughened Polyamide 6/Polypropylene Nanocomposites

M. U. WAHIT, A. HASSAN,
Z. A. MOHD ISHAK, A. R. RAHMAT,
and N. OTHMAN

[Regular Article]
Vol. 38, No. 8, pp 767–780 (2006)

The effect of rubber type and functionality on the morphological and mechanical properties of rubber-toughened polyamide 6/polypropylene nanocomposites containing organophilic modified montmorilonite (OMMT) was investigated in term of mechanical testing, X-ray diffraction (XRD) and scanning electron microscopy (SEM) Malaysian_hungary Bilateral Program. The toughness of the nanocomposites toughened by maleated elastomer was higher than the unmaleated elastomer. The SEM observation revealed that rubber functionality reduces the elastomer particle size in the PA6/PP matrix due to the *in situ* formation of graft copolymer between maleated elastomer and PA6.

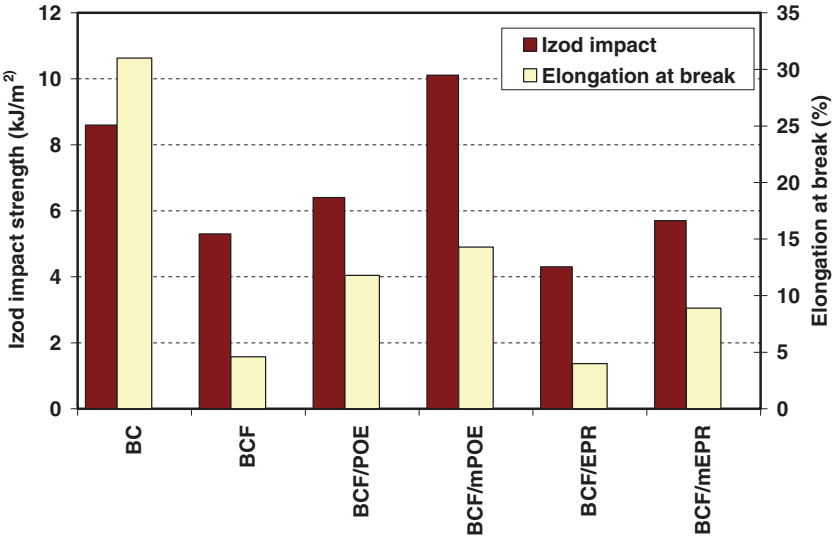

Significant Effect of Dopant Size on Nanoscale Fractal Structure of Polypyrrole Film

A. EFTEKHARI, M. KAZEMZAD, and M. KEYANPOUR-RAD

[Regular Article]
Vol. 38, No. 8, pp 781–785 (2006)

Surface morphologies of thin films of polypyrrole doped with two similar anions (with different ionic radii) *viz.* chloride and bromide were compared by means of fractal geometry. Scanning electron micrographs of the polymer surfaces showed a significant difference between the surface structures of two anion-doped polypyrrole films in microscale and particularly in nanoscale. Surprisingly, the bromide-doped polypyrrole had nanostructure; whereas, the chloride-doped polypyrrole surface was smooth in nanoscale. An electrochemical method based on gold-masking approach was employed to reveal the fractality of these polymer surfaces in microscale.

Chloride- and bromide-doped polypyrrole films

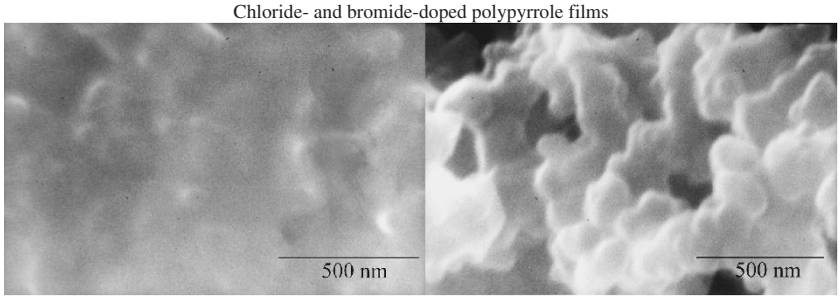

Size Shrinkage of Methacrylate-based Terpolymer Latexes Synthesized by Free Radical Polymerization: Kinetics and Influence of Main Reaction Parameters

S. ARMINI, C. M. WHELAN, M. SMET, S. ESLAVA, and K. MAEX

[Regular Article]
Vol. 38, No. 8, pp 786–798 (2006)

Monodisperse PMMA-based terpolymer particles are synthesized with a wide and controllable range of size and polymer content by emulsifier-free free radical emulsion polymerization. The effect of monomer amount, reaction temperature and initiator concentration is investigated. A kinetic study of the evolution of the terpolymer colloid composition and morphology reveals a mechanism of fast homogeneous nucleation. The composition of the particles changes continuously during the polymerization, giving rise to a spectrum of polymer properties promising for a number of unique applications.

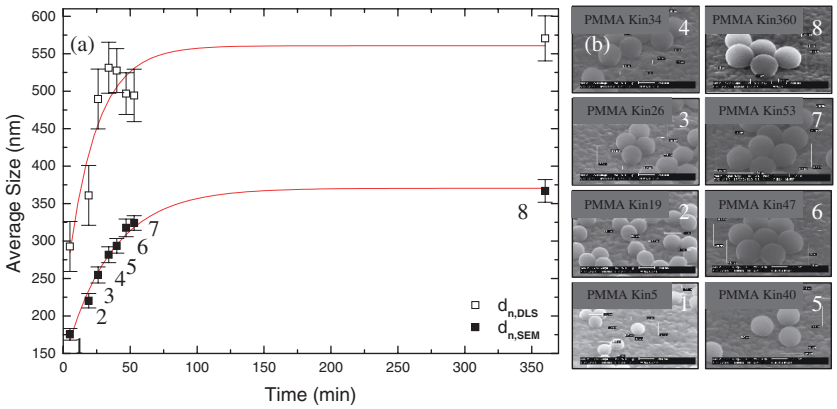

Effect of Soft Segments of Waterborne Polyurethane on Organic Vapor Sensitivity of Carbon Black Filled Waterborne Polyurethane Composites

B. ZHAO, R. W. FU, M. Q. ZHANG, H. YANG, M. Z. RONG, and Q. ZHENG

[Regular Article]
Vol. 38, No. 8, pp 799–806 (2006)

Three types of waterborne polyurethane (WPU) with different soft segments were synthesized. The WPUs were then compounded with carbon black to fabricate gas sensing composites. By studying the composites' resistance variation in different solvent-vapors, it was found that the structures of the WPUs remarkably affected the composites' response behaviors. Both polarity and flexibility of the soft segments of WPU determine the solvent-polymer interaction and preferential localization of solvent and fillers, resulting in different magnitudes of resistance increase and rates of response.

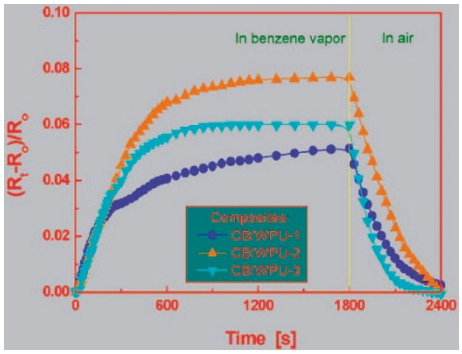

Polymer Grafting onto Carbon Black by Solid State Method

H. XU, B. LI, and C. WU

[Regular Article]
Vol. 38, No. 8, pp 807–813 (2006)

In situ grafting of natural rubber (NR) onto the CB surface by solid state method was investigated in this paper. The torque value of CB/NR blend system in Haake internal mixer and FT IR spectra of grafted carbon black (GCB) illuminated that the grafting reaction took place. The orthogonal design (ORD) showed that the degradation time of NR and mixing temperature played an important role in the grafting process. The mechanical properties of vulcanized NR filled with GCB were enhanced to a large extent.

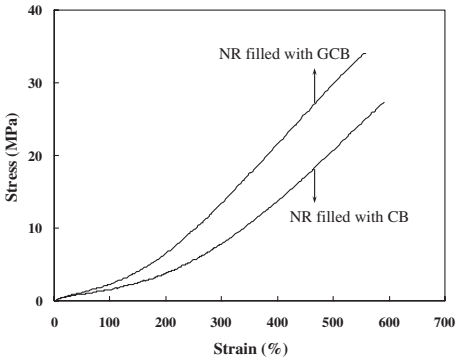

Physical Aging and Refractive Index of Poly(methyl methacrylate) Glass

N. TANIO and T. NAKANISHI

[Regular Article]
Vol. 38, No. 8, pp 814–818 (2006)

Physical aging of poly(methyl methacrylate) (PMMA) glass was studied by refractive index measurement. We measured change of refractive index of PMMA glass with annealing at temperatures below the glass transition temperature (T_g) by optical prism coupling, and determined volume relaxation by physical aging using the Lorentz-Lorenz equation. In this paper, the effect of aging temperature on volume relaxation of PMMA glass was investigated. Maximum volume relaxation for PMMA glass was determined at 20 °C below the T_g.

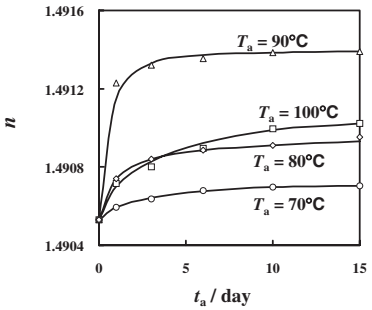

Figure Refractive index (n) at 633 nm plotted as a function of aging time (t_a) at various aging temperature (T_a) for PMMA glass.

Two Different Surface Properties of Regenerated Cellulose due to Structural Anisotropy

C. YAMANE, T. AOYAGI, M. AGO,
K. SATO, K. OKAJIMA,
and T. TAKAHASHI

[Regular Article]
Vol. 38, No. 8, pp 819–826 (2006)

High planar orientation index f(1-10) and high crystallinity X_c values yielded significantly lower contact angles. Water contact angle of *ca.* 12° is far lower than that of widely used polymers. Because of the density of hydroxyl groups on the (1-10) surface is very high, higher X_c and f(1-10) values resulting in a larger surface area fraction of (1-10) planes in regenerated cellulose films produce the most hydrophilic polymer, more wettable than PVA and starch.

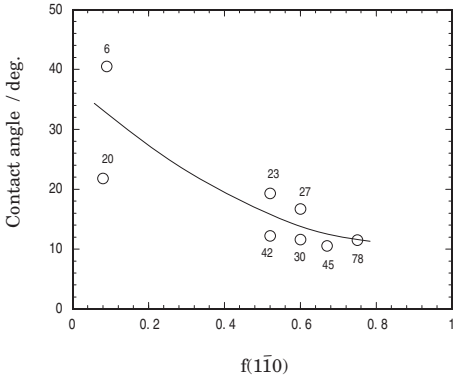

Relation between (1-10) plane orientation index f(1-10) and contact angle for water. Numbers denote crystallinity Xc.

Positive-type Alkaline Developable Photosensitive Branched Polyamides with Low Degree of Branching and Diazonaphthoquinone as a Photosensitive Compound

J. XIAO, Y. INAI, L. LI, T. HAYAKAWA, and M. KAKIMOTO

[Regular Article]
Vol. 38, No. 8, pp 827–834 (2006)

A positive-type photosensitive polyamide based on the branched polyamides with low degree of branching (DB) and diazonaphthoquinone (S-DNQ) as a photosensitive compound has been developed. The branched polyamides with low DB having phenolic hydroxy end groups were prepared by through polycondensation of ABB′ type monomer and subsequently end-modification of the branched polyamides having amino end groups obtained. A fine positive image of 6 μm line-and-space pattern was obtained when the film was exposed to 300 mJ cm^{-2} by contact-printing mode.

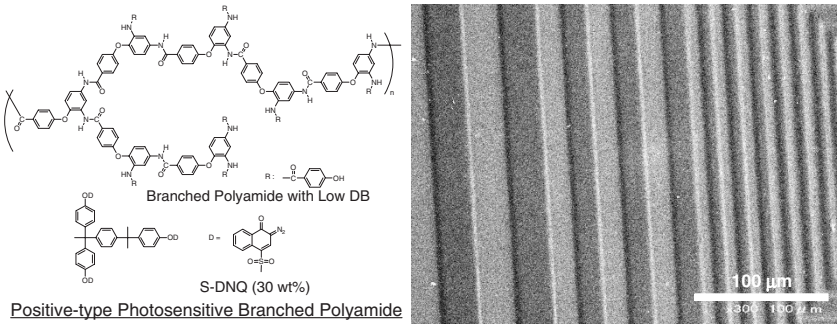

***In Situ* Polymerization and Properties of Methyl Methacrylate-Butadiene-Styrene Resin with Bimodal Rubber Particle Size Distribution**

J. TAKAHASHI, H. WATANABE, J. NAKAMOTO, K. ARAKAWA, and M. TODO

[Regular Article]
Vol. 38, No. 8, pp 835–843 (2006)

In situ polymerization and mechanical properties of rubber-modified MBS resin with a bimodal rubber particle size distribution were investigated. Rubber-modified MBS resin was prepared by bulk-suspension polymerization. Bimodal rubber particle size distribution was observed during bulk polymerization. Size distribution was regulated by the viscosity of prepolymer or shearing. MBS resin with bimodal distribution (Sample code D-2) was superior in balance of impact resistance and transparency.

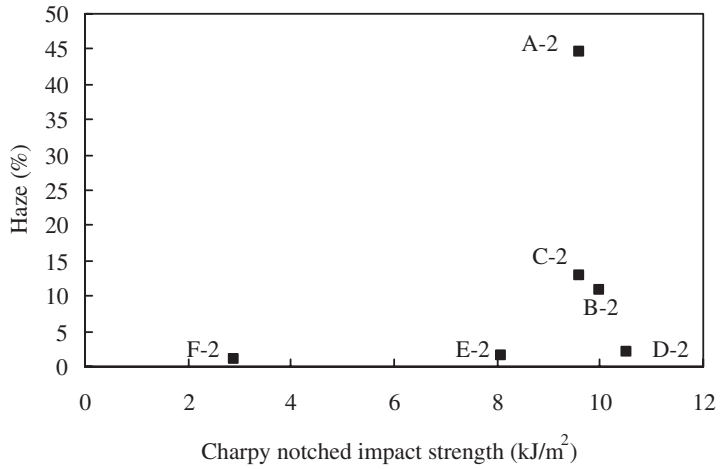

Preparation of Antibacterial Polymer-grafted Nano-sized Silica and Surface Properties of Silicone Rubber Filled with the Silica

R. YAMASHITA, Y. TAKEUCHI, H. KIKUCHI, K. SHIRAI, T. YAMAUCHI, and N. TSUBOKAWA

[Regular Article]
Vol. 38, No. 8, pp 844–851 (2006)

The grafting of polymeric phosphonium salt, poly(St-$SO_3^-P^+Bu_3R$), onto the silica surface was achieved by the treatment of poly(*p*-styrene sodium sulfate) [poly(St-$SO_3^-Na^+$)] with tributyltetradecylphosphonium chloride ($Bu_3RP^+Cl^-$). The poly(St-$SO_3^-P^+Bu_3R$)-grafted silica gave a stable dispersion in DMSO and poly(dimethylsiloxane). It was found that silicone rubber filled with the poly(St-$SO_3^-P^+Bu_3R$)-grafted silica shows extremely strong antibacterial activity. The silicone rubber surface has an ability to inhibit the reproduction of a *Staphylococcus aureus* and an *Escherichia coli*.

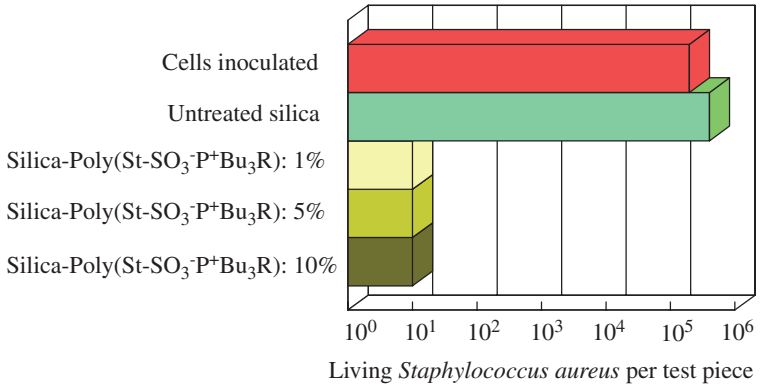

Synthesis of Star-shaped 8 arms Poly(ethylene glycol)-Poly(L-lactide) Block Copolymer and Physicochemical Properties of Its Solution Cast Film as Soft Biomaterial

K. NAGAHAMA, Y. OHYA, and T. OUCHI

[Regular Article]
Vol. 38, No. 8, pp 852–860 (2006)

Star-shaped 8 arms PEG-*b*-PLLA was synthesized to create the novel implantable soft material. The 8 arms PEG-*b*-PLLA films showed drastically lower crystallinity of PLLA compared with the corresponding linear 2 arms PEG-*b*-PLLA film. The homogeneously fine PLLA domains were formed in the 8 arms PEG-*b*-PLLA film, whereas the miscellaneous PLLA domains were formed in the 2 arms PEG-*b*-PLLA film. Consequently, the 8 arms PEG-*b*-PLLA film showed higher water absorption ability and lower tensile strength as well as higher elongation at break than the 2 arms PEG-*b*-PLLA film.

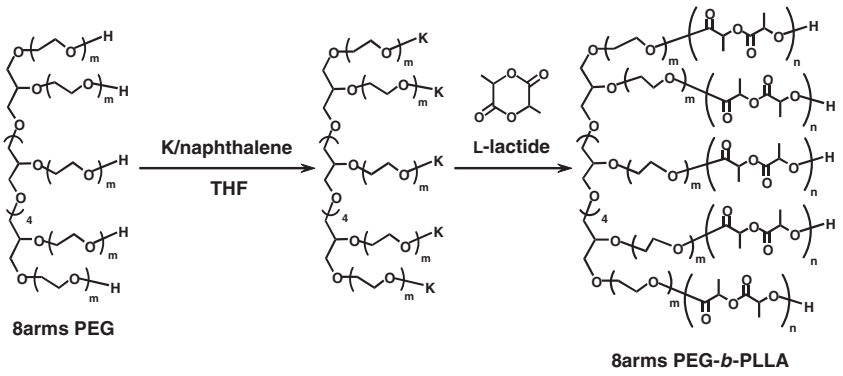

Electrostatic Contributions to Chain Stiffness and Excluded-Volume Effects in Sodium Poly(2-acrylamido-2-methylpropanesulfonate) Solutions

R. HAGINO, J. YASHIRO, M. SAKATA, and T. NORISUYE

[Regular Article]
Vol. 38, No. 8, pp 861–867 (2006)

The electrostatic persistence length q_{el} and the excluded-volume strength B for Na poly(2-acrylamido-2-methylpropanesulfonate) in aqueous NaCl at 25 °C are estimated as functions of salt concentration C_s by analysis of intrinsic viscosity data based on the wormlike chain with excluded volume. It is shown that, as was the case for Na poly(styrenesulfonate), available polyelectrolyte theories fail to describe the C_s-dependence of the estimated q_{el} and B.

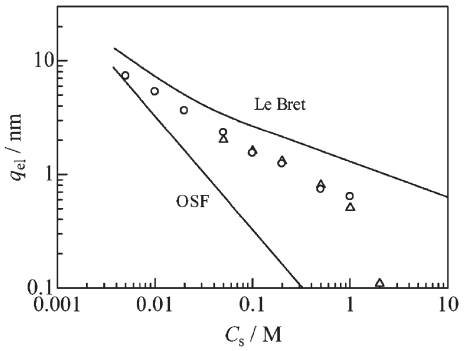

Morphology of Segmented Polyether Based Poly(urea-urethane) Thermoplastic Elastomers

J.-Y. LIU, Y.-C. HSU, and Y.-Z. WANG

[Regular Article]
Vol. 38, No. 8, pp 868–875 (2006)

A series of aniline-containing segmented poly(urea-urethane) were prepared as a conductive material. An amine-terminated functional group was introduced into the poly(urea-urethane) as a chain extender to form the hard segment of the copolymer. The conductivity of copolymers is found to be ranged from 0.83 S/cm for the neat OPA to 1.96×10^{-6} S/cm for the resultant copolymers. TEM and CP experiments results indicate that morphology of conducting copolymers undergo microphase separation and the domain size is on a nanophase scale.